Editors' Suggestion

Nonlocal optical potential in inelastic deuteron scattering off ^{24}Mg

A. Deltuva* and D. Jurčiukonis
Institute of Theoretical Physics and Astronomy, Vilnius University, Saulėtekio al. 3, LT-10257 Vilnius, Lithuania

(Received 7 April 2023; accepted 16 May 2023; published 6 June 2023)

Nonlocal nucleon-nucleus optical potential with rotational quadrupole deformation enabling the excitation of the ^{24}Mg(2^+) state is developed; it fits well the proton-^{24}Mg elastic and inelastic differential cross section in the beam energy range from 30 to 45 MeV per nucleon. The inelastic deuteron-^{24}Mg scattering leading to the excited ^{24}Mg(2^+) state is studied in the same energy regime by solving the three-body Faddeev-type equations for transition operators. Effects of the optical potential nonlocality are evaluated by comparison with local models. Significant effects on the inelastic differential cross section are found at forward angles up to the first peak and at larger angles beyond the second peak. Nonlocal optical potential provides a simultaneous reasonable reproduction of the experimental data for the elastic and inelastic proton-^{24}Mg and deuteron-^{24}Mg scattering not achieved using local potentials.

DOI: 10.1103/PhysRevC.107.064602

I. INTRODUCTION

In a recent study of deuteron stripping and pickup reactions [1] we united two important ingredients beyond the widely employed standard nuclear dynamics, namely, the nonlocal extension of the nucleon-nucleus potentials and the excitation of the nuclear core. Furthermore, we used rigorous three-body Faddeev-type equations for transition operators [2,3] and obtained accurate solutions in the momentum-space partial-wave framework. The achieved description of the experimental data and the consistency between the two-body and three-body description is considerably improved as compared to previous studies.

Encouraged by the above-mentioned success, in the present work we aim to investigate the interplay of the optical potential nonlocality and the collective nuclear degrees of freedom, i.e., the nuclear core excitation (CeX), yet in another type of reactions, the inelastic deuteron scattering. To the best of our knowledge, the importance of the nonlocality in this reaction type is unexplored so far since it necessitates the CeX which in previous studies was always assumed to have a local form. We take the ^{24}Mg nucleus as a working example, since (i) its lowest states display rather well the rotational band structure describable by the quadrupole deformation, (ii) the experimental differential cross section data are available not only for elastic and inelastic scattering of deuterons [4], but also for the elastic and inelastic nucleon-nucleus scattering [5], which is necessary to constrain the potentials, and (iii) several quite sophisticated theoretical calculations using local potentials already exist. They are based on the extension of the continuum discretized coupled channels (CDCC) method [6,7] and the Faddeev-type theory [8]. As pointed out there, the two-body distorted-wave Born approximation (DWBA), though able to fit the experimental data [4], requires values for the quadrupole deformation parameter β_2 that are inconsistent with the nucleon-nucleus data. The consistency was partially improved by using three-body treatments such as CDCC or Faddeev, though definite conclusions were precluded by the shortcomings of the used optical potentials. The results in Refs. [7,8] were obtained with global optical potential parametrizations such as Chapel Hill 89 (CH89) [9] and Koning and Delaroche (KD) [10], that provide reasonable but not perfect description of the nucleon-^{24}Mg scattering data. One of our goals in the present work is the development of nonlocal optical potentials with an improved account of the two-body data. Furthermore, while some parameters of local optical potentials are energy dependent, the nonlocal form exhibits a weaker energy dependence and therefore a good fit of the experimental data over a broader energy range is possible with energy-independent parameters, thereby allowing to reduce the ambiguities and increase the predictive power of the nonlocal optical potential [1].

In Sec. II we recall the three-body Faddeev formalism, while in Sec. III we develop nonlocal optical potentials and, for comparison, local ones. In Sec. IV we present analysis and discussion of the deuteron-^{24}Mg scattering observables, with conclusions summarized in Sec. V.

II. THREE-PARTICLE EQUATIONS WITH NUCLEAR EXCITATION

We consider the three-particle system of a proton (p), a neutron (n), and a nuclear core with the mass number A, the latter being ^{24}Mg in the considered case. The version of three-particle Faddeev equations [2] for transition operators, directly related to scattering amplitudes, was proposed by Alt, Grassberger, and Sandhas (AGS) [3]. Extended to include the excitation of one of the particles, the nucleus A in the present case, the AGS equations for multicomponent

*arnoldas.deltuva@tfai.vu.lt

transition operators $U^{cb}_{\gamma\beta}$ read

$$U^{cb}_{\gamma\beta} = \bar{\delta}_{\gamma\beta}\,\delta_{cb}(G^c_0)^{-1} + \sum_{\alpha=p,n,A}\sum_{a=g,x}\bar{\delta}_{\gamma\alpha}\,T^{ca}_{\alpha}\,G^a_0 U^{ab}_{\alpha\beta}. \quad (1)$$

Here, the Latin superscripts label the internal states of the nucleus, either the ground (g) state ^{24}Mg(0^+) or the excited (x) state ^{24}Mg(2^+) with 1.369 MeV excitation energy (we do not include higher excited states of ^{24}Mg), and the Greek subscripts label the spectator particle in the odd-man-out notation, e.g., the spectator p implies the pair A+n, etc. Furthermore, $\bar{\delta}_{\gamma\beta} = 1 - \delta_{\gamma\beta}$, G^a_0 is the free resolvent in the respective Hilbert sector a, and

$$T^{ca}_{\alpha} = V^{ca}_{\alpha} + \sum_{b=g,x} V^{cb}_{\alpha} G^b_0 T^{ba}_{\alpha} \quad (2)$$

is the two-particle transition operator. For A+n and A+p pairs it couples the two Hilbert sectors as the respective potential V^{ca}_{α} does, since the nucleus A can be excited/de-excited when interacting with nucleons.

The amplitude for the deuteron inelastic scattering is determined by the transition operator component U^{xg}_{AA}, which is, however, coupled to the other five components $U^{cg}_{\gamma A}$ via the AGS equations (1). In Ref. [8] all those equations for transition operator components are given explicitly, together with the description of asymptotic channel states, the Coulomb treatment via the screening and renormalization method, and the relation to the differential cross section. The AGS equations are solved in the momentum-space partial-wave representation, employing three different sets of basis states, as appropriate for the treatment of three interacting pairs of particles. Further technical details of calculations are described in Ref. [8] and references therein.

III. NONLOCAL POTENTIAL

In our transition-operator integral-equation formalism the nonlocal coordinate-space potentials V^{ca}_{α}, transformed into the momentum space representation, do not require any special treatment as compared to local ones. As in Ref. [1] we start with a single-particle nonlocal coordinate-space potential

$$\langle \mathbf{r}'|V_N|\mathbf{r}\rangle = \tfrac{1}{2}[V(r')H(|\mathbf{r}'-\mathbf{r}|) + H(|\mathbf{r}'-\mathbf{r}|)V(r)], \quad (3)$$

where $\mathbf{r}$ and $\mathbf{r}'$ are initial and final distances between particles, $V(r)$ is local potential function of the respective distance, and

$$H(x) = \pi^{-3/2}\rho^{-3}e^{-(x/\rho)^2} \quad (4)$$

is the nonlocality function with the nonlocality range ρ. As argued in Ref. [1], this phenomenological form is closely related to the Perey and Buck potential [11], and in the limit $\rho \to 0$ one obviously recovers the local potential $V(r)$. We parametrize $V(r)$ in the same way as done for standard optical potentials [9,10], i.e.,

$$V(r) = -V_V\,f_V(r) - iW_V\,f_W(r) - i4W_S\,f_S(r)[1-f_S(r)] + V_s\frac{2}{r}\frac{df_s(r)}{dr}\,\boldsymbol{\sigma}\cdot\mathbf{L}. \quad (5)$$

The four terms with strength parameters V_V, W_V, W_S, and V_s, correspond to the real volume, imaginary volume, imaginary surface, and real spin-orbit contributions, respectively. Their radial dependence is modeled by the standard Woods-Saxon functions

$$f_j(r) = \frac{1}{1+e^{(r-R_j)/a_j}} \quad (6)$$

with parametric dependence on the radius R_j and diffuseness a_j.

The potential given by Eqs. (3)–(6) does not act on internal degrees of freedom of the nucleus A and therefore does not induce its excitation/de-excitation. This can be achieved by its deformation [12–14]. The rotational model, quite consistent with the low-energy spectrum of ^{24}Mg, assumes a permanent quadrupole deformation of ^{24}Mg . This effectively results in the Woods-Saxon radius $R_j = R_{j0}[1 + \beta_2 Y_{20}(\hat{\xi})]$, where β_2 is the quadrupole deformation parameter and $\hat{\xi}$ describes the internal nuclear degrees of freedom in the body-fixed frame [8,13,14]. For calculations in the partial-wave representation the deformed potential has to be expanded into multipoles. In addition to the central contribution $\lambda = 0$ one has to include also the $\lambda = 2$ multipole to induce the transitions between 0^+ and 2^+ states of ^{24}Mg [7,8,13,14]. In the coordinate-space partial-wave basis $|rLSJ\rangle$, where L, S, and J denote the two-particle relative orbital momentum, the total spin S, and the conserved total angular momentum J, respectively, the two functions $H(|\mathbf{r}'-\mathbf{r}|)$ and $V(r)$ are transformed separately, and then combined into a nonlocal potential

$$\langle r'L'S'J|V^{ca}_N|rLSJ\rangle = \tfrac{1}{2}\big[V^{ca}_{L'S',LS,J}(r')H_L(r',r) + H_{L'}(r',r)V^{ca}_{L'S',LS,J}(r)\big]. \quad (7)$$

Here,

$$H_L(r',r) = 2\pi\int_{-1}^{1} dx P_L(x)\,H(\sqrt{r'^2+r^2-2r'rx}) \quad (8)$$

is the partial-wave projection of $H(|\mathbf{r}'-\mathbf{r}|)$, with $P_L(x)$ being the Legendre polynomial, and $V^{ca}_{L'S',LS,J}(r)$ is the standard local potential with the CeX [13,14], whose $c \neq a$ components arise from the $\lambda = 2$ multipole and couple different internal states of the nucleus A. A local potential of this type has been used also in previous calculations of deuteron-^{24}Mg scattering [7,8].

Finally, the transformation of the potential (7) to the momentum space, as required for our calculations, is straightforward, i.e.,

$$\langle p'L'S'J|V^{ca}_N|pLSJ\rangle = (-1)^{\frac{L'-L}{2}}\frac{2}{\pi}\int_0^\infty dr'\,dr\,r'^2r^2\,j_{L'}(p'r') \times \langle r'L'S'J|V^{ca}_N|rLSJ\rangle\,j_L(pr), \quad (9)$$

where p is the relative nucleon-nucleus momentum, and $j_L(x)$ is the spherical Bessel function of the order L. For the proton-nucleus interaction the Coulomb contribution, including the deformation [8,13], is added.

The values of the optical potential parameters have to be obtained by fitting the experimental data. We are interested in deuteron-^{24}Mg scattering at 30 to 45 MeV/nucleon beam energies [4], and the elastic and inelastic $p + ^{24}$Mg data in this

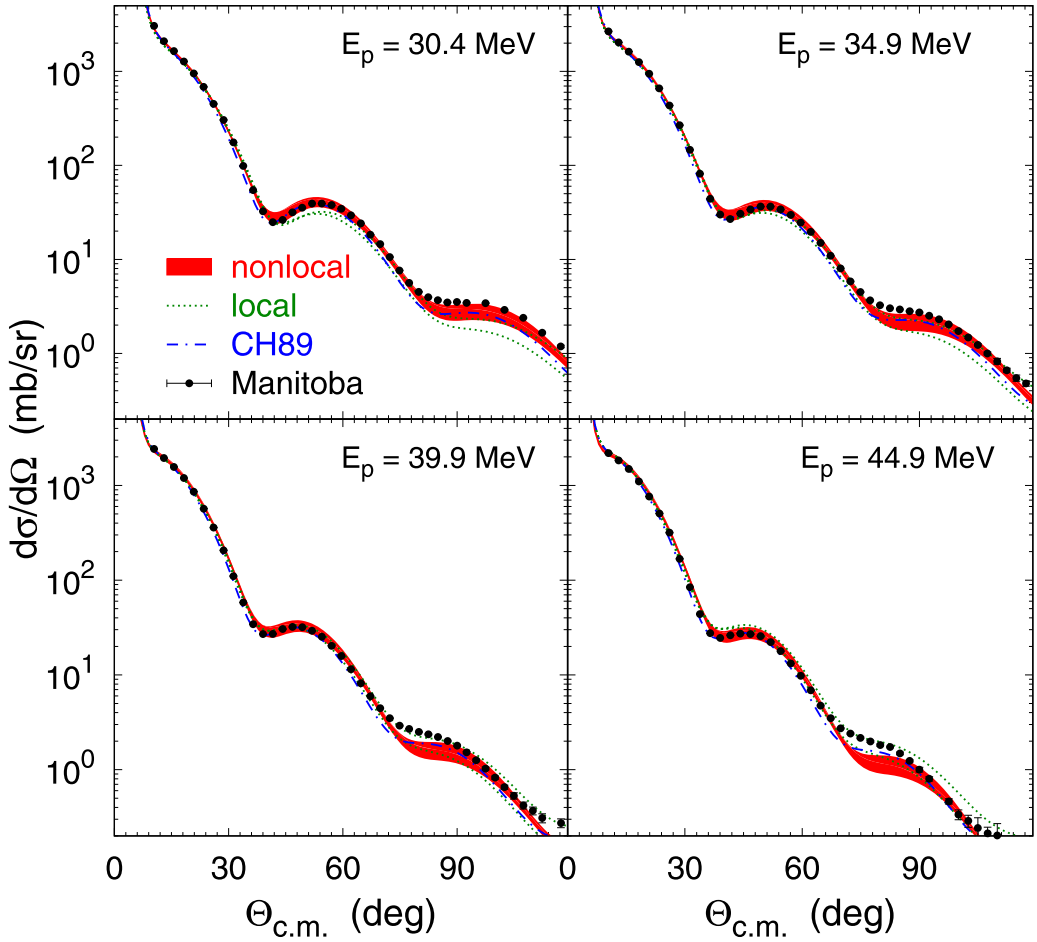

FIG. 1. Differential cross section for elastic $p + {}^{24}$Mg scattering at beam energies $E_p = 30.4$, 34.9, 39.9, and 44.9 MeV. Results obtained with different parameter sets of the nonlocal optical potential are combined into bands, while curves represent predictions based on local potentials, i.e., those developed in this work (dotted lines) and CH89 (dashed-dotted lines). The experimental data from Ref. [5] were measured at University of Manitoba.

energy regime is available [5]. The data for the $n + {}^{24}$Mg reaction are quite scarce and only available at lower energies. On the other hand, ^{24}Mg is an isospin symmetric $Z = N$ nucleus, consequently, after separation of the Coulomb contributions, the nuclear parts of the proton and neutron optical potentials should be similar, as it is the case for global parametrizations [9,10,15]. We therefore take the optical potential parameters for the neutron-nucleus to be those for the proton-nucleus.

One could consider the strengths, radii and diffuseness for the four terms in Eq. (5) plus β_2 and ρ as fit parameters. However, for a fair comparison with previous results we demand that the number of free parameters in our potential does not exceed the one in standard optical potentials, and introduce additional constrains: (i) the nonlocality range is fixed to $\rho = 1$ fm, a typical value for nonlocal potentials [1,15,16]; (ii) geometric parameters for both volume and surface imaginary terms are chosen to be the same, i.e., $R_W = R_S$ and $a_W = a_S$, as it is often the case for standard parametrizations [9]; (iii) since polarization observables are not studied, and cross sections are insensitive to the spin-orbit interaction, it is not subjected to the fit and not deformed. Instead, we assume $R_s = R_{V0}$, $a_s = a_V$, and $V_s = 7.5$ MeV fm^2, consistently with the polarization data for ^{16}O [1]. With these constrains our fitting parameters are β_2, V_V, W_W, W_S, a_V, a_W, r_V and r_W, where the reduced radii r_j are related to Woods-Saxon radii in the standard way $R_{j0} = r_j A^{1/3}$.

We fit simultaneously differential cross section for elastic and inelastic $p + {}^{24}$Mg scattering at beam energies $E_p = 30.4$, 34.9, 39.9, and 44.9 MeV [5]. In order to achieve a better fit at smaller angles, relevant for the deuteron scattering, we exclude the data at center-of-mass angles $\Theta_{\rm c.m.}$ beyond 70°. We estimate the uncertainties by developing a number of parameter sets that fit the data with a comparable quality; several typical examples are collected in Table I. The quadrupole deformation parameter β_2 takes the values from 0.50 to 0.57, i.e., with spread of nearly 15%, but the deformation length $\delta_2 = \beta_2 R_{V0}$ varies within 5% only, ranging from 1.56 to 1.64 fm. The corresponding predictions for $p + {}^{24}$Mg elastic and inelastic scattering to the 2^+ state are displayed as bands in Figs. 1 and 2, and agree reasonably well with the experimental data [5].

In order to evaluate importance of the optical potential nonlocality, we attempted to fit the same data with $\rho = 0$, i.e., using an energy-independent local potential. The local

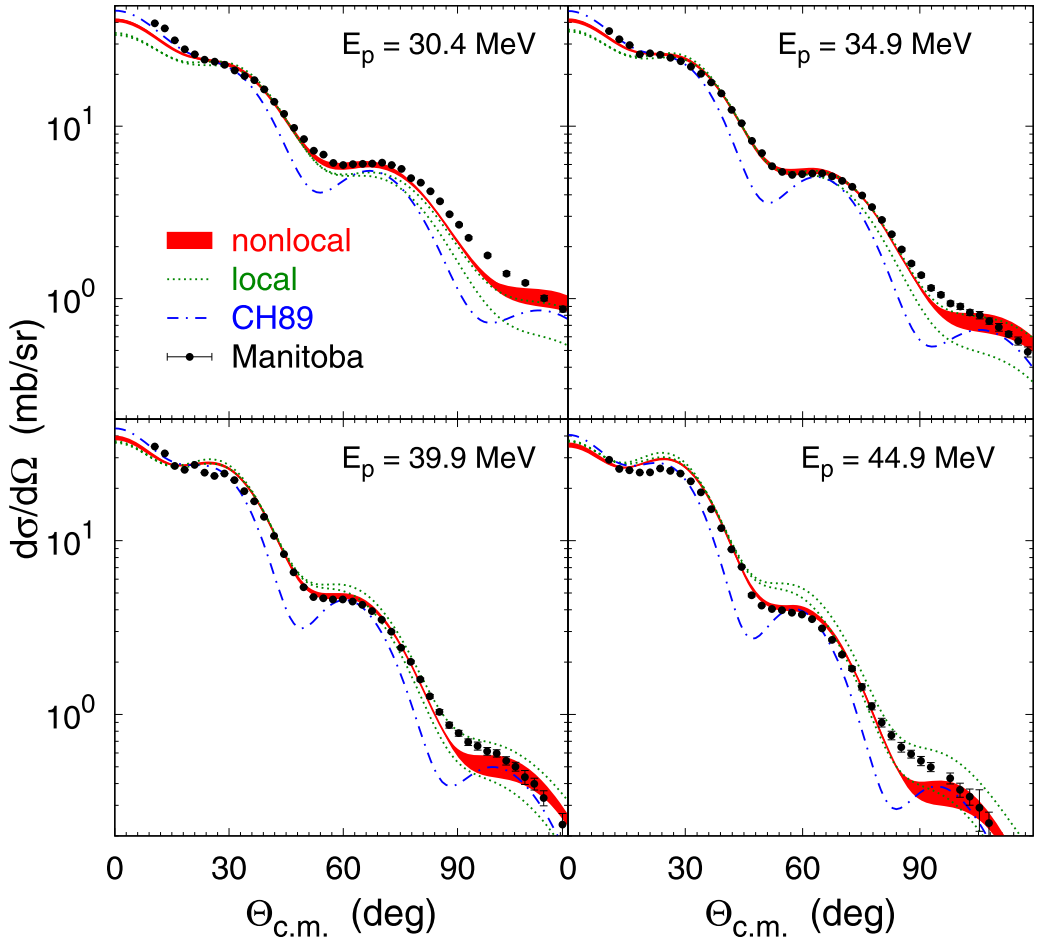

FIG. 2. Differential cross section for inelastic $p + {}^{24}$Mg scattering leading to the ^{24}Mg(2^+) state. Results at beam energies $E_p = 30.4$, 34.9, 39.9, and 44.9 MeV are shown. Bands, curves, and experimental data are as in Fig. 1.

model has the same constrains as nonlocal one, except that $V_s = 6.0\,\text{MeV fm}^2$, a typical value for local potentials. As expected, such a potential is less successful in a broader energy range, the deviations from the data are most evident for the lowest and highest considered energy. For each observable we present in Figs. 1 and 2 two dotted curves, their difference may provide some estimation of uncertainties. The deduced values for $\beta_2 = 0.52$ and 0.55 are consistent with nonlocal cases, while for $\delta_2 = 1.73$ and 1.77 fm they are slightly larger. In addition, as dashed-dotted curves we include the predictions based on the global optical potential parametrization CH89 [9], deformed with $\beta_2 = 0.5$ and $\delta_2 = 1.69$ fm and already used in previous studies [7,8]. This potential has energy-dependent parameters. It reproduces reasonably well the elastic differential cross section but fails for inelastic data at $\Theta_{\text{c.m.}} > 40^\circ$, having a different shape of the angular distribution. Thus, the optical potentials developed in the present work yield a significant improvement in the description of inelastic $p + {}^{24}$Mg scattering.

TABLE I. Five example sets for nonlocal $p + {}^{24}$Mg optical potential parameters with $\rho = 1$ fm. The strengths V_V, W_W, and W_S are in MeV, while r_j, a_j, and δ_2 are in fm.

V_V	W_W	W_S	r_V	r_W	a_V	a_W	β_2	δ_2
106.64	7.76	6.84	1.01	1.10	0.70	0.67	0.54	1.57
100.75	7.25	9.80	1.07	1.09	0.66	0.56	0.50	1.56
101.28	8.01	9.73	1.05	1.03	0.67	0.61	0.52	1.60
105.34	7.46	7.37	1.02	1.04	0.68	0.75	0.53	1.58
108.79	7.39	8.66	0.99	1.03	0.69	0.70	0.57	1.64

IV. RESULTS FOR THREE-BODY REACTION

We proceed to the analysis of ^{24}Mg(d, d') differential cross sections at deuteron beam energies $E_d = 60$, 70, 80, and 90 MeV, as measured at Jülich Research Center [4]. Solution of the three-body AGS equations with the quadrupole excitation of the ^{24}Mg nucleus requires three pair potentials as input. The proton-nucleus and neutron-nucleus optical potentials are taken from the previous section; as there, the proton-nucleus interaction is appended with central and deformed Coulomb terms. The neutron-proton interaction is modeled with a realistic CD Bonn potential [17].

In Fig. 3 we present the calculated differential cross sections for the ^{24}Mg(d, d') reaction with the final ^{24}Mg nucleus

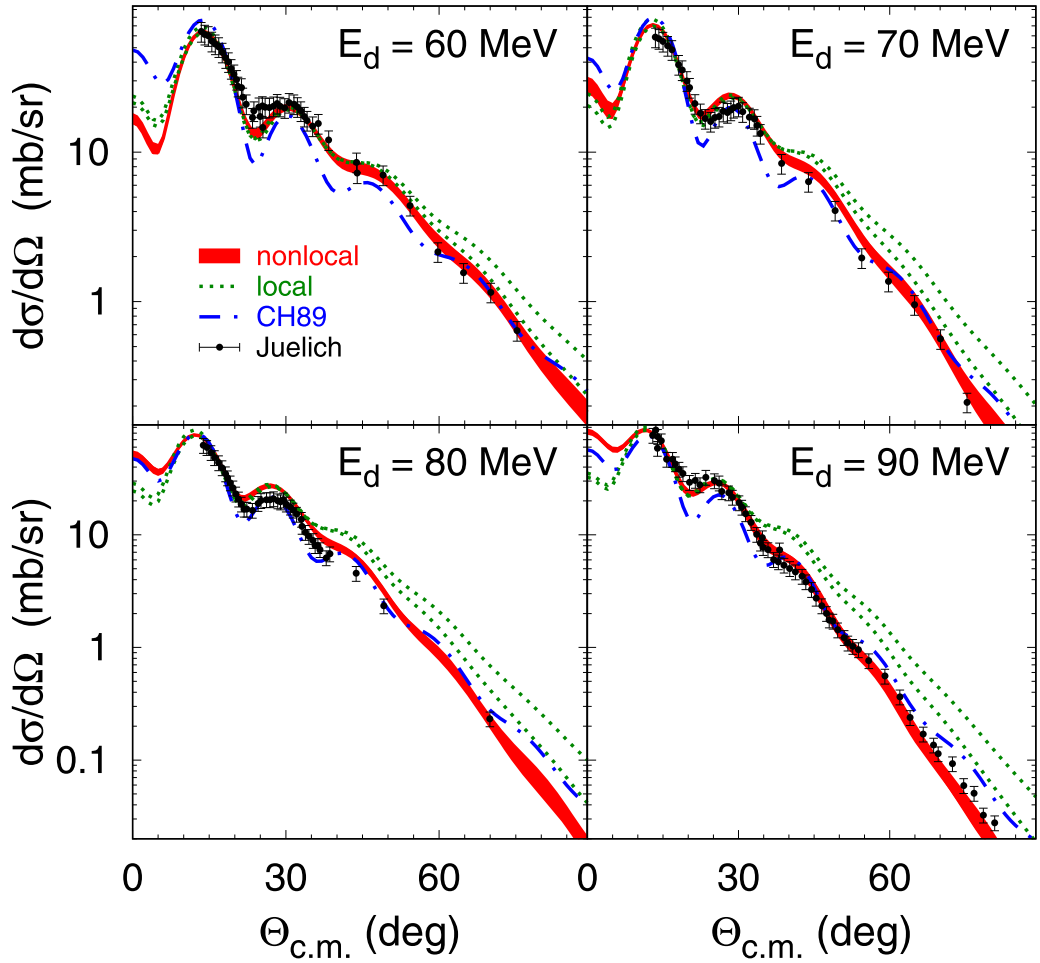

FIG. 3. Differential cross section for inelastic $d + {}^{24}$Mg scattering leading to the ^{24}Mg(2^+) state. Results at deuteron beam energies E_d = 60, 70, 80, and 90 MeV are shown. Bands and curves are as in Fig. 1. The experimental data from Ref. [4] were measured at Jülich Research Center.

being in its first excited state 2^+. The predictions obtained with nonlocal potentials are displayed as bands, those with local potentials as dotted curves, and those based on the CH89 are shown as dashed-dotted curves. The comparison of different calculations and experimental data lead to the following important observations:

(i) The CH89-based differential cross sections exhibit minima near $\Theta_{\text{c.m.}} = 20$ and 40 degrees that are considerably deeper than those seen in data and other calculations. This is likely a consequence of a similar discrepancy seen in the ^{24}Mg(p, p') inelastic scattering in Fig. 2 near $\Theta_{\text{c.m.}} = 50$ and 90 degrees. Thus, the failure of the CH89 model around the minima can be explained by the shortcomings present already at the two-body level.

(ii) The first peak near $\Theta_{\text{c.m.}} = 15^\circ$ is best reproduced by the band of nonlocal optical potentials, with slight overprediction at 70 and 80 MeV. The local models, especially CH89 at 60 and 70 MeV, show larger overprediction. This difference has no evident explanation at the two-body level.

(iii) Both local and nonlocal models, fitted in this work to proton-nucleus data, mutually agree quite well around the second peak, that moves from 30 to 25 degrees with increasing beam energy. The agreement with data is quite good at 60 and 90 MeV, but overprediction up to 20% is observed at 70 and 80 MeV. In contrast, the CH89 provides a better agreement at 70 and 80 MeV, but underpredicts the data at 60 and 90 MeV. The energy evolution is smooth for the predictions but not for the data points, raising some concerns regarding their accuracy.

(iv) Predictions using nonlocal optical potentials describe the experimental data well also at large scattering angles while local models clearly overpredict the data. This again finds no explanation by looking back into the nucleon-nucleus scattering, as there the local model predictions may be even below those of nonlocal models and data, as happens in Fig. 2 at $E_p = 30.4$ MeV.

(v) All three types of employed models predict different energy evolution of the differential cross section at forward angles $\Theta_{\text{c.m.}} < 10^\circ$ below the first peak, with no evident explanation at the two-body level. Unfortunately, no experimental data is available in this angular regime.

We also would like to discuss several uncertainties related to the above study and argue that the main conclusions remain unaffected.

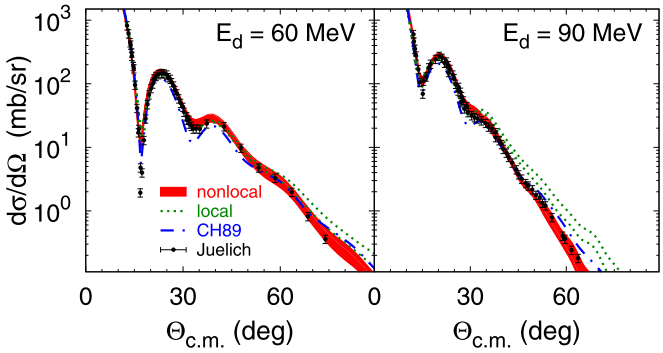

FIG. 4. Differential cross section for elastic $d + {}^{24}$Mg scattering at 60 and 90 MeV deuteron beam energy. Bands, curves, and experimental data are as in Fig. 3.

(a) Changing the nonlocality parameter ρ by $\pm 10\%$ and refitting other parameters does not change visibly the description of two- and three-body data shown in Figs. 1–3 for $\rho = 1$ fm. Changes in the spin-orbit force only become visible at large angles, beyond the scale of Figs. 1–3.

(b) At $E_p = 30$ MeV we developed single-energy local potential fitting proton-^{24}Mg data as good as nonlocal models do. Nevertheless, the three-body results follow closely the trend of local models in Fig. 2

(c) Since global optical potentials such as CH89 have both proton-nucleus and neutron-nucleus parametrizations, we verified the effect of using proton-nucleus parameters for the neutron-nucleus pair. The effect turns out to be visible only at very small angles, reaching 5% at $\Theta_{\rm c.m.} = 0^\circ$ but decreasing to roughly 1% at the first peak and beyond it.

(d) We included only the first excited state 2^+ of ^{24}Mg, while the CDCC-type calculations [7] investigated the effect of the second excited state 4^+ and found up to 7% reduction of the $^{24}\mathrm{Mg}(d, d')$ differential cross section, most visible at the first peak. However, one has to keep in mind that the inclusion of the 4^+ state changes also the $^{24}\mathrm{Mg}(p, p')$ predictions. In principle, one should refit the potential parameters, otherwise also the $^{24}\mathrm{Mg}(p, p')$ cross section is slightly decreased and the observed effect in the $^{24}\mathrm{Mg}(d, d')$ reaction is partially caused by changes in $^{24}\mathrm{Mg}(p, p')$. As the refitting was not performed in Ref. [7], the real effect of the 4^+ state is expected to be less significant.

The nonlocality effect in the deuteron-nucleus elastic scattering has been investigated previously [18], as it does not demand including the nuclear excitation. Therefore we show in Fig. 4 the $^{24}\mathrm{Mg}(d, d)$ differential cross section at lowest and highest considered energy only. Despite different nucleus and more elaborated optical potentials of the present work, the nonlocality effect appears to be qualitatively similar to the one observed in Ref. [18] for the elastic deuteron scattering off ^{16}O and ^{40}Ca nuclei. As compared to local models, the nonlocal ones predict lower differential cross section at intermediate and large angles, and this change is clearly favored by the experimental data, as can be seen in Fig. 4 as well.

V. CONCLUSIONS

We studied the effect of the optical potential nonlocality in the inelastic deuteron-nucleus scattering. ^{24}Mg nucleus with the excited 2^+ state was chosen as a working example. We developed a nonlocal nucleon-nucleus optical potential with rotational quadrupole deformation, coupling ground and excited states, and fitted to proton-^{24}Mg elastic and inelastic differential cross section. A good reproduction of data in the 30 to 45 MeV range was achieved with energy-independent parameters; several parameter sets were determined to estimate the uncertainties. The local models, especially the CH89 potential used in earlier calculations, are less successful in reproducing experimental proton-^{24}Mg data.

We described the elastic and inelastic deuteron-nucleus scattering using rigorous three-body Faddeev-type equations for transition operators, and solved them in the momentum-space partial-wave representation. Differential cross sections were calculated at deuteron beam energies 60 to 90 MeV. Using nonlocal models we obtained a good description of the inelastic experimental data, the overprediction of the second peak at 70 and 80 MeV may point to the inconsistency of the data sets at different energies. The results based on the global CH89 potential fail in the minima regions, which can be explained by the shortcomings of the potential in the nucleon-nucleus system. The most visible effects of the optical potential nonlocality occur at forward angles up to the first peak and at larger angles beyond the second peak. While in the former case the experimental data are not available, in the latter case nonlocal models are clearly favored over the local ones. These differences have no evident explanation in the nucleon-nucleus system. We also argued that simplification assumptions such as using the same parameters for proton and neutron optical potentials and neglecting higher excited states are not expected to change the conclusions.

Finally, the nonlocality effect in the elastic deuteron-nucleus scattering is consistent with previous studies of other nuclei. It reduces the differential cross section at larger angles improving the agreement with the experimental data.

In summary, using nonlocal optical potentials we obtained a simultaneous satisfactory reproduction of the experimental data for elastic and inelastic proton-^{24}Mg and deuteron-^{24}Mg scattering, not achieved in previous studies. A new measurement at forward angles could provide even more stringent test.

ACKNOWLEDGMENT

This work was supported by Lietuvos Mokslo Taryba (Research Council of Lithuania) under Contract No. S-MIP-22-72.

[1] A. Deltuva and D. Jurčiukonis, Phys. Lett. B **840**, 137867 (2023).

[2] L. D. Faddeev, Zh. Eksp. Teor. Fiz. **39**, 1459 (1960) [Sov. Phys. JETP **12**, 1014 (1961)].

[3] E. O. Alt, P. Grassberger, and W. Sandhas, Nucl. Phys. B **2**, 167 (1967).
[4] A. Kiss, O. Aspelund, G. Hrehuss, K. Knopfle, M. Rogge, U. Schwinn, Z. Seres, P. Turek, and C. Mayer-Boricke, Nucl. Phys. A **262**, 1 (1976).
[5] D. K. Hasell, N. E. Davison, T. N. Nasr, B. T. Murdoch, A. M. Sourkes, and W. T. H. van Oers, Phys. Rev. C **27**, 482 (1983).
[6] P. Chau Huu-Tai, Int. J. Mod. Phys. E **20**, 953 (2011).
[7] M. Gómez-Ramos and A. M. Moro, Phys. Rev. C **95**, 034609 (2017).
[8] A. Deltuva, Nucl. Phys. A **947**, 173 (2016).
[9] R. L. Varner, W. J. Thompson, T. L. McAbee, E. J. Ludwig, and T. B. Clegg, Phys. Rep. **201**, 57 (1991).
[10] A. J. Koning and J. P. Delaroche, Nucl. Phys. A **713**, 231 (2003).
[11] F. Perey and B. Buck, Nucl. Phys. **32**, 353 (1962).
[12] A. Bohr and B. R. Motelson, *Nuclear Structure* (World Scientific, Singapore, 1998).
[13] T. Tamura, Rev. Mod. Phys. **37**, 679 (1965).
[14] I. J. Thompson, Comput. Phys. Rep. **7**, 167 (1988).
[15] M. M. Giannini and G. Ricco, Ann. Phys. **102**, 458 (1976).
[16] M. M. Giannini, G. Ricco, and A. Zucchiatti, Ann. Phys. **124**, 208 (1980).
[17] R. Machleidt, Phys. Rev. C **63**, 024001 (2001).
[18] A. Deltuva, Phys. Rev. C **79**, 021602(R) (2009).